PROCEEDINGS OF SCIENCE

Diphoton production in the ADD model to NLO+PS accuracy

M. K. Mandal,[a] **P. Mathews**[*,b] **V. Ravindran,**[c] **S. Seth**[b]

[a] *Regional Centre for Accelerator-based Particle Physics, Harish-Chandra Research Institute, Allahabad 211 019, India*

[b] *Saha Institute of Nuclear Physics, 1/AF Bidhan Nagar, Kolkata 700064, India*

[c] *The Institute of Mathematical Sciences, Tharamani, Chennai 600 113, India*

We present next-to-leading order predictions for the diphoton production in the ADD model, matched to the HERWIG parton shower using the MC@NLO formalism. A selection of results is presented for $d = 2 - 6$ extra dimensions, using generic cuts as well as analysis cuts mimicking the search strategies as pursued by the CMS experiment.

11th International Symposium on Radiative Corrections (Applications of Quantum Field Theory to Phenomenology) (RADCOR 2013),
22-27 September 2013
Lumley Castle Hotel, Durham, UK

[*] Speaker.

PoS(RADCOR 2013)030

1. Introduction

The large extra dimension model (ADD) [1] is an important new physics scenario at the TeV scale that addresses the hierarchy problem and is being extensively studied at the LHC. ATLAS [2] and CMS [3] for the 7 TeV pp collision, have looked for evidence of extra spatial dimensions in the diphoton production and put bounds on the fundamental Planck scale M_S in $(4+d)$-dimensions.

As a result of the graviton propagating in the extra dimensions, its 4-dimensional realisation in the ADD model corresponds to a tower of KK modes. Interaction of the massive spin-2, KK modes $h_{\mu\nu}^{(\vec{n})}$ with the standard model (SM) particles localised on a 3-brane, is *via* the energy momentum tensor $T^{\mu\nu}$ of the SM

$$\mathscr{L} = -\frac{\kappa}{2}\sum_{(\vec{n})} T^{\mu\nu}(x)h_{\mu\nu}^{(\vec{n})}(x), \tag{1.1}$$

where $\kappa = \sqrt{16\pi}/M_P$ and M_P is the Planck mass in 4-dimensions. In process involving virtual exchange of KK modes between the SM particles, the sum of the KK mode propagator $\mathscr{D}(s)$ is given by

$$\kappa^2\mathscr{D}(s) \;=\; \kappa^2\sum_n \frac{1}{s-m_n^2+i\varepsilon} = \frac{8\pi}{M_S^4}\left(\frac{\sqrt{s}}{M_S}\right)^{(d-2)}\left[-i\pi+2I\left(\frac{\Lambda}{\sqrt{s}}\right)\right], \tag{1.2}$$

where d is the compactified extra spatial dimensions, s is the partonic center of mass energy, Λ is the UV cutoff of the KK mode sum which is usually identified as M_S [4, 5] and the integral $I(\Lambda/Q)$ is given in [4]. We have included the κ^2 suppression as a result of gravity coupling in Eq. 1.2, which on summation over the high multiplicity of KK modes compensates the suppression in the ADD model.

Next to leading order (NLO) QCD corrections in some of the pair production processes are substantial in the ADD model and their inclusion leads to reduction in the theoretical uncertainties, making it possible for the experiments to put more stringent bounds on the extra dimension model parameters. Improved theoretical predictions to higher orders in QCD have been performed for pair production processes *viz.* di-lepton [6], di-gauge boson ($\gamma\gamma$ [7], ZZ and W^+W^- [8]), which in extra dimension models could result from the exchange of a virtual KK mode in addition to the usual SM contribution. The real emission of KK modes leads to large missing E_T signal *viz.* mono-jet [9], mono-photon [10], mono-Z boson, and mono-$W^\pm$ boson [11].

Quantitative impact of NLO QCD corrections to the diphoton final state for extra dimension searches has been studied in [7], where various infrared safe observables were studied using phase space slicing method. The factorisation scale dependence gets reduced when $\mathscr{O}(\alpha_s)$ corrections are included. Fixed order calculation truncated to NLO, at best yields results for sufficiently inclusive observable. For the ADD model, matching fixed order NLO diphoton results with parton shower Monte Carlo (PS), according to the MC@NLO method [12], has been done in [13], where the coverage of the kinematical region has been extended to consistently include resummation in the collinear limit and also provide a more exclusive description of the final state to make it as realistic as possible to the experimental situation. The diphoton final state is an important signal for extra dimension searches, as the branching ratio of a KK mode decay to diphoton is twice than that of a decay to individual charged lepton pair.

ATLAS [2] and CMS [3] have analysed the diphoton invariant mass spectrum, using a constant K-factor for the full range of the invariant mass distribution to put lower bounds on extra dimension scale to NLO accuracy. However, this choice is not sensitive to possible distortions of distributions that can arise at NLO. In this analysis, we have considered various distributions for the ADD model parameters $d = 2$ to 6 with appropriate M_S value as bounded by the experiments [2, 3], to NLO+PS accuracy. Factorisation, renormalisation scale uncertainties and PDF uncertainties are also estimated in an automated way [14].

2. NLO + PS

Since the KK modes couple universally to the SM particles through the energy momentum tensor, both the $q\bar{q}$ and gg channel would contribute to the diphoton final state at leading order (LO). In the SM, the gg channel starts only at next to next to leading order (NNLO) *via* the finite box contribution through quark loop and the large gluon-gluon flux at the LHC makes this contribution potentially comparable to the LO results. In the invariant mass region of interest to extra dimension searches, the box diagram contribution is not significant enough [7].

For the ADD model, all the partonic contributions to NLO in QCD have been calculated for the diphoton final state [7]. QCD radiative corrections through virtual one loop gluon and real emission of gluons to the $q\,\bar{q} \to \gamma\,\gamma$ subprocess, would contribute to both SM and extra dimension models. The $q(\bar{q})\; g \to q(\bar{q})\; \gamma\,\gamma$ begins to contribute for both SM and extra dimension models at NLO. The LO $g\;g \to \gamma\;\gamma$ extra dimension process will also get one loop virtual gluon and real gluon emission radiative corrections. There will also be interference between the SM and extra dimension model to give contributions up to $\mathcal{O}(\alpha_s)$. In this analysis, we have not included the $\mathcal{O}(\alpha_s)$ corrections as a result of the interference between the SM box diagram contribution and LO extra dimension contribution to the $g\;g \to \gamma\;\gamma$ subprocess, as it is quite suppressed in the region of interest to extra dimension models [7]. The term we have neglected contributes only about 0.1% to the gg subprocess. All other interference terms between the SM and ADD model to order $\mathcal{O}(\alpha_s)$ have been included.

The $q(\bar{q})\; g \to q(\bar{q})\; \gamma\,\gamma$ NLO contribution has an additional QED collinear singularity when the photon gets collinear to the emitting quark and can be absorbed into the fragmentation function which gives the probability of a parton fragmenting into a photon. Parton fragmentation functions are additional non perturbative inputs which are not very well known. At the LHC, secondary photons as a result of hadron decaying into collinear photons and jets faking as photon are taken care of by photon isolation criteria [2, 3] which also substantially reduces the fragmentation contribution. Since the fragmentation is essentially a collinear effect, the fragmentation function can be avoided by the smooth cone isolation [15], which ensures that in no region of the phase space the soft radiation is eliminated. The smooth cone isolation is able to eliminate the not so well known fragmentation contribution and at the same time, ensures infrared safe (IR) observable.

For the implementation of the smooth cone isolation, a cone is defined centered in the direction of the photon in the pseudo rapidity (η) and azimuthal angle (ϕ) plane, with radius $r = \sqrt{(\eta-\eta_\gamma)^2+(\phi-\phi_\gamma)^2}$. The hadronic activity $H(r)$ is defined as the sum of hadronic transverse energy in a circle of radius $r < r_0$. For all cones with $r \leq r_0$ the isolation criterion $H(r) < H(r)_{\max}$

has to be satisfied, where $H(r)_{\max}$ is defined as

$$H(r)_{\max} = \varepsilon_\gamma E_T^\gamma \left(\frac{1-\cos r}{1-\cos r_0} \right)^n , \tag{2.1}$$

where E_T^γ is the transverse energy of the photon and the nature of the function $H(r)_{\max}$ depends on the parameters $0 < \varepsilon_\gamma < 1$ and n a positive integer. Consequently, closer to the photon the hadronic activity diminishes and for the collinear configuration there is no hadronic activity. It is hence able to get rid of the fragmentation contribution and at the same time the observable defined is infrared safe.

We have chosen to work in the aMC@NLO framework [16], which automatises the MC@NLO formalism [12] to match NLO computations with parton showers. In this paper we present results matched to HERWIG6 [17]. For the NLO computation, isolation of IR poles from the real part and phase space integrations are carried out by MadFKS [18], which automatises the FKS subtraction method [19] using the MadGraph [20] matrix-element generator, whereas for one-loop amplitudes the results of Ref. [7] are used. The automation within the MadGraph framework requires a new HELAS [21] subroutine to calculate helicity amplitudes with massive spin-2 particles [22, 23]. In addition, for our present analysis, we have implemented the sum over the KK modes to take care of the virtual KK mode sum (Eq. 1.2) that contributes to process in the ADD model [23]. We use this framework to generate the events for 8 TeV run at the LHC. For the invariant mass distributions, we have reproduced the fixed order results of [7] using the fixed order results from MadFKS. Also numerical cancellation of the singularities from the real and virtual terms have been explicitly checked.

3. Numerical results

The following input parameters are used: $\alpha_{em}^{-1} = 132.507$, $G_F = 1.16639 \times 10^{-5}$ GeV^{-2}, $m_Z = 91.188$ GeV. Our calculation is LO in the electroweak coupling and therefore, the dependence on the scale in this coupling constant is beyond the precision of our results. In our electroweak scheme, m_W and $sin^2\theta_W$ are computed from m_Z, α_{em} and G_F (this value for the α_{em} gives a W-boson mass ($m_W = 80.419$ GeV) that is close to the experimental value). We use MSTW2008(n)lo68cl for (N)LO parton distribution functions (PDF) [24]. The MSTW PDF also sets the value of the strong coupling $\alpha_s(m_Z)$ at LO and NLO in QCD. The renormalisation and factorisation scales are chosen as $\mu_F = \mu_R = M_{\gamma\gamma}$, the invariant mass of the photon pair. The events that have to be showered are generated using the following generation cuts: $|\eta_{\gamma_{1,2}}| < 2.6$, $p_T^{\gamma_{1,2}} > 20$ GeV, diphoton invariant mass 100 GeV $< M_{\gamma\gamma} < M_S$ and the photon isolation is done using the Frixione isolation with $r_0 = 0.38$, $\varepsilon_\gamma = 1$ and $n = 2$ (see Eq. (2.1)). More specific analysis cuts can be applied subsequently to generate the events.

The dependence of the prediction of an observable on the factorisation and renormalisation scales is a result of the uncalculated higher order contributions, which can be estimated by varying μ_F and μ_R independently around the central value $\mu_F = \mu_R = M_{\gamma\gamma}$. The variation is done by the following assignment $\mu_F = \xi_F\ M_{\gamma\gamma}$ and $\mu_R = \xi_R\ M_{\gamma\gamma}$, where the values of (ξ_F, ξ_R) used are (1,1), (1/2,1/2), (1/2,1), (1,1/2), (1,2), (2,1), (2,2). The various ratios of μ_F, μ_R and $M_{\gamma\gamma}$ that appear as arguments of logarithms in the perturbative expansion to NLO are within the range [1/2,2]. The

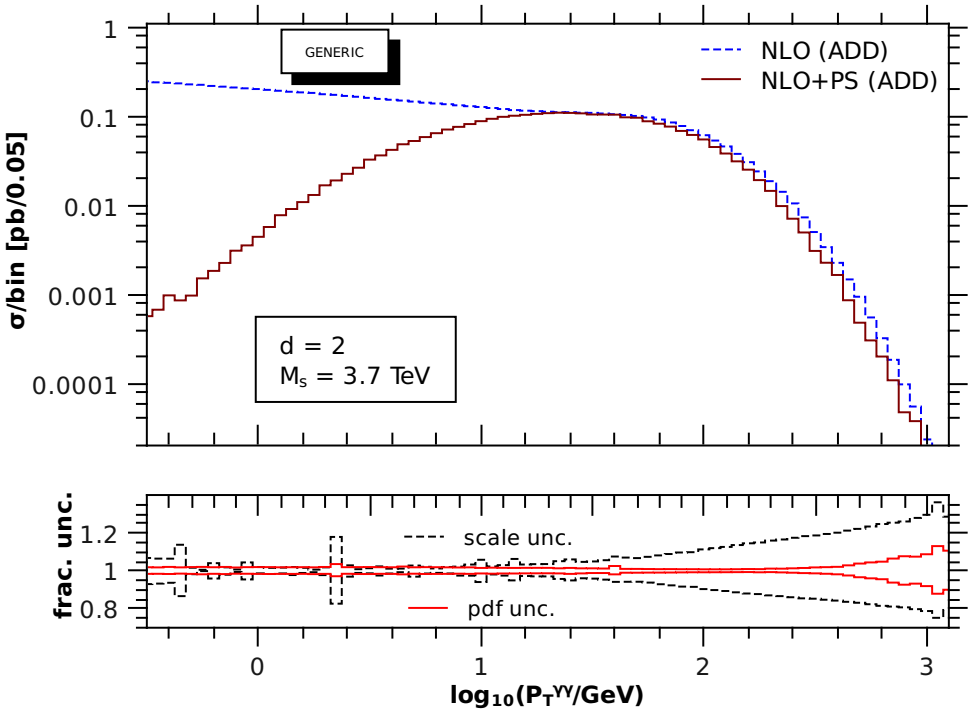

Figure 1: Transverse momentum distribution $p_T^{\gamma\gamma}$ of the diphoton for the fixed order NLO and NLO+PS. The ADD model parameters used are $d = 2$ and $M_S = 3.7$ TeV. The lower inset displays the scale and PDF, fractional uncertainties for the NLO+PS results.

variation of both μ_F and μ_R are taken as the envelope of the above individual variations. Variation of only μ_F would involve the choice $\xi_R = 1$ and varying ξ_F and vice-versa for variation of only μ_R. The PDF uncertainties are estimated using the prescription given by MSTW [24]. Fractional uncertainty, defined as the ratio of the variation about the central value divided by the central value, is a good indicator of the scale and PDF uncertainties and is plotted in the lower insets to the various figures.

To begin with, we compare the fixed order NLO result with NLO+PS for the transverse momentum of the diphoton ($\log_{10} p_T^{\gamma\gamma}$) using generic cuts: $M_{\gamma\gamma} > 140$ GeV, $|\eta_\gamma| < 2.5$, $p_T^{\gamma_1} > 40$ GeV, $p_T^{\gamma_2} > 25$ GeV and $r_0 = 0.4$. In Fig. 1, $\log_{10} p_T^{\gamma\gamma}$ distribution is plotted for $d = 2$ with appropriate M_S value. It is clear that at low $p_T^{\gamma\gamma}$ values, NLO+PS correctly resums the Sudakov logarithms, leading to a suppression of the cross section, while the fixed order NLO results diverges for $p_T^{\gamma\gamma} \to 0$. At high $p_T^{\gamma\gamma}$, the NLO fixed order and NLO+PS results are in agreement. In the lower inset of the Fig. 1, we have scale and PDF variation to NLO+PS, which increase with $p_T^{\gamma\gamma}$. The $p_T^{\gamma\gamma}$ distribution is in reality a LO result, while in the low $p_T^{\gamma\gamma}$ region the parton shower effects include higher order effects, thereby reducing the scale dependence in that region (Fig. 1).

We now present the results for the various kinematical distributions to NLO+PS accuracy, for analysis specific cuts. CMS have looked for diphoton invariant mass in the region 140 GeV $< M_{\gamma\gamma} < M_S$. For CMS, the corresponding cuts are [3]: $|\eta_\gamma| < 1.44$, $p_T^\gamma > 70$ GeV, photon isolation: (i) sum of the energy of hadrons $\sum E(H) < 0.05 E^\gamma$ with $\Delta r < 0.15$, (ii) sum of transverse energy

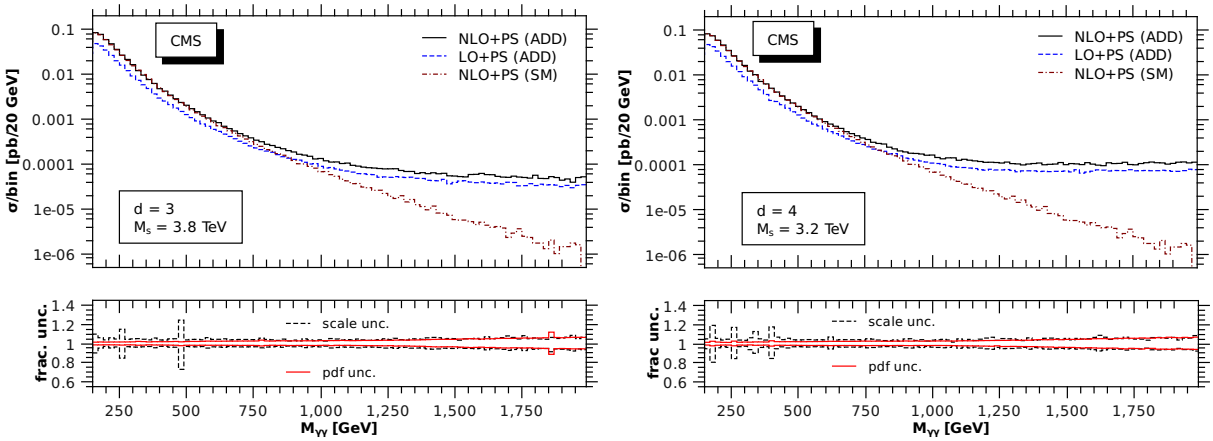

Figure 2: Invariant mass distribution for $d = 3$ (left panel) and $d = 4$ (right panel) is plotted for ADD and SM contributions to NLO+PS accuracy. The lower insets gives the corresponding scale and PDF, fractional uncertainties for NLO+PS (ADD).

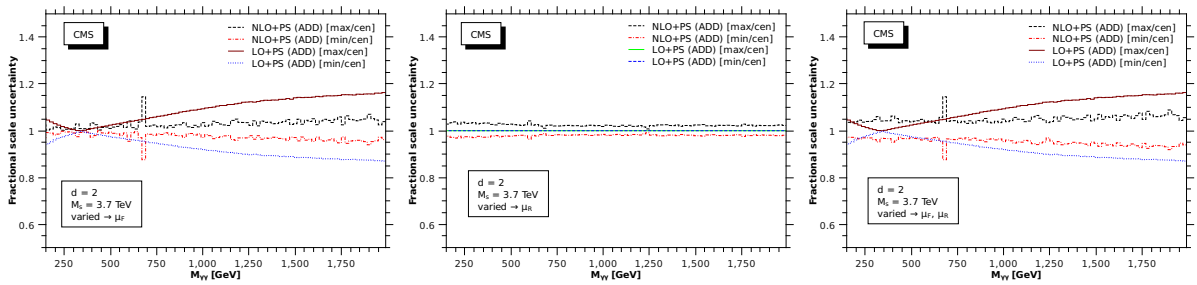

Figure 3: For the invariant mass distribution, with $d = 2$ and $M_S = 3.7$ TeV, the fractional uncertainties as a result of μ_F variation (left panel), μ_R variation (central panel) and μ_F, μ_R variation (right panel).

of hadrons $\sum E_T(H) < 2.2\ \text{GeV} + 0.0025\, E_T^{\gamma}$ with $0.15 < \Delta r < 0.4$. In addition to the CMS photon isolation, if we also include the Frixione isolation criteria, there is no appreciable change in the results.

In Fig. 2, the corresponding invariant mass distributions for $d = 3, 4$ are plotted using CMS cuts. The choice of M_S used for the plots corresponds to the lower bounds obtained by [2, 3] using the diphoton process. By including higher order corrections, the scale dependence goes down from about 25% at LO, to about 10% at NLO. The PDF uncertainty does not change significantly and remains about 8%.

We now consider the fractional scale uncertainties on the invariant mass distribution as a result of the variation of the scales μ_F and μ_R (both independently and simultaneously) in going from LO+PS to NLO+PS. Note that the LO cross sections depend only on μ_F through the PDF sets, but at NLO level the scale μ_R enters through $\alpha_s(\mu_R)$ and $\log(\mu_F/\mu_R)$ coming from the partonic cross sections after mass factorisation. As expected the inclusion of NLO QCD correction reduces the factorisation scale dependence resulting from the LO observable which is clear from Fig. 3 (left panel). In the high $M_{\gamma\gamma}$ region, the uncertainty of about 25% at LO+PS gets reduced to 5% when

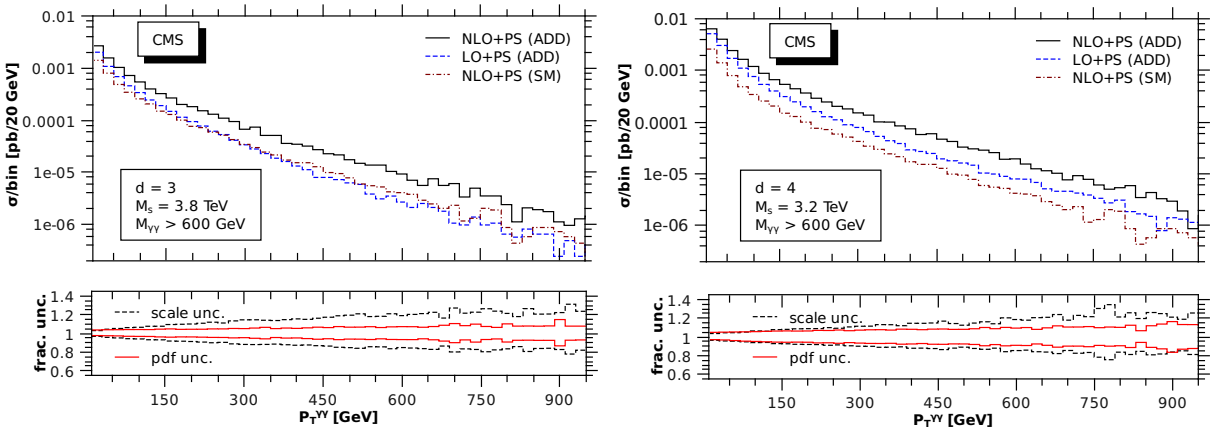

Figure 4: The transverse momentum distribution $p_T^{\gamma\gamma}$ of the diphoton for $d = 3$ (left panel) and $d = 4$ (right panel).

NLO+PS corrections are included. On the other hand, the μ_R dependence enters only at NLO level (see middle panel of Fig. 3) which will get reduced only if NNLO corrections are included. Hence, we see our NLO corrections are sensitive to the choice of μ_R but the variation is only 5% and is fairly constant for the range of invariant mass considered. If we vary both μ_F and μ_R simultaneously as shown in Fig. 3 (right panel), we find that the reduction in the μ_F scale dependence at NLO level is mildly affected by the μ_R variation in the large invariant mass region. In the small invariant mass region, the LO and NLO results exhibit smaller μ_F dependence compared to the large invariant mass region. But μ_R dependence coming from the NLO results does not change much with the invariant mass $M_{\gamma\gamma}$. Hence variation due to μ_R at small $M_{\gamma\gamma}$ is larger compared to that resulting from μ_F. This explains the behavior at small invariant mass regions where the NLO+PS variation is in excess of the LO+PS (see right panel of Fig. 3).

Finally, we plot the transverse momentum distribution in Fig. 4 for $d = 3$ (left panel) and $d = 4$ (right panel), for the SM and ADD model to NLO+PS accuracy, with $M_{\gamma\gamma} > 600$ GeV. The ADD results are also plotted for LO+PS. The scale and PDF uncertainties are displayed as insets at the bottom of the plots for NLO+PS (ADD). Additional results can be found in [13].

4. Conclusion

In this analysis, we have presented the diphoton final state production in the large extra dimension model to NLO in QCD and matching to parton shower is implemented using the aMC@NLO framework. All the subprocesses that contribute to the diphoton final state from both the SM and ADD model are considered to NLO in QCD. Using a set of generic cuts we first demonstrated the importance of NLO+PS over the fixed order NLO computations, by considering the $p_T^{\gamma\gamma}$ distribution. We have presented our results for various observables *viz.*, invariant mass and transverse momentum of the diphoton, to NLO+PS accuracy. It is important to note that there is substantial enhancement of the various distributions due to the inclusion of NLO corrections and both the theoretical and PDF uncertainties have been estimated. There is a significant decrease in theoretical uncertainties from over 20% at LO to about 10% when NLO corrections are included. The codes

needed to generate the events for the diphoton final states to NLO+PS accuracy are available on the website http://amcatnlo.cern.ch.

Acknowledgement:
The authors would like to thank collaborators R. Frederix, P. Torrielli and M. Zaro for valuable comments and discussions. The work of MKM and VR has been partially supported by funding from Regional Center for Accelerator-based Particle Physics (RECAPP), Department of Atomic Energy, Govt. of India.

References

[1] N. Arkani-Hamed, S. Dimopoulos and G. Dvali, Phys. Lett. B 429 (1998) 263; I. Antoniadis, N. Arkani-Hamed, S. Dimopoulos and G. Dvali, Phys. Lett. B 436 (1998) 257; N. Arkani-Hamed, S. Dimopoulos and G. Dvali, Phys. Rev. D59 (1999) 086004.

[2] ATLAS Collaboration, Phys. Lett. B710 (2012) 538.

[3] CMS Collaboration, arXiv: 1112.0688 [hep-ex]

[4] T. Han, J. D. Lykken and R. J. Zhang, Phys. Rev. D59 (1999) 105006

[5] G. F. Giudice, R. Rattazzi, and J. D. Wells, Nucl. Phys. B544 (1999) 3.

[6] P. Mathews, V. Ravindran, K. Sridhar and W. L. van Neerven, Nucl. Phys. B713 (2005) 333; P. Mathews, V. Ravindran, Nucl. Phys. B753 (2006) 1; M.C. Kumar, P. Mathews, V. Ravindran, Eur. Phys. J. C49 (2007) 599.

[7] M.C. Kumar, *et. al.* Phys. Lett. B672 (2009) 45; Nucl. Phys. B818 (2009) 28.

[8] N. Agarwal, *et. al.* Nucl. Phys. B 830, 248 (2010); Phys. Rev. D 82, 036001 (2010).

[9] S. Karg, M. Karamer, Q. Li, and D. Zeppenfeld, Phys. Rev. D 81, 094036 (2010).

[10] X. Gao, C. S. Li, J. Gao, and J. Wang, Phys. Rev. D 81, 036008 (2010).

[11] M.C. Kumar, *et. al.* Nucl. Phys. B847, 54 (2011); J. Phys. G 38, 055001 (2011).

[12] S. Frixione, B. R. Webber, JHEP 06 (2002) 029.

[13] R. Frederix, *et. al.* JHEP 1212 (2012) 102.

[14] R. Frederix, S. Frixione, V. Hirschi, F. Maltoni, R. Pittau and P. Torrielli, JHEP 02 (2012) 099.

[15] S. Frixione, Phys. Lett. B 429, 369 (1998).

[16] R. Frederix, S. Frixione, V. Hirschi, F. Maltoni, R. Pittau, P. Torrielli, Phys. Lett. B701 (2011) 427.

[17] G. Corcella, *et. al.* JHEP 01 (2001) 010.

[18] R. Frederix, S. Frixione, F. Maltoni, T. Stelzer JHEP 0910 (2009) 003.

[19] S. Frixione, Z. Kunszt, and A. Signer, Nucl. Phys. B467 (1996) 399.

[20] J. Alwall, M. Herquet, F. Maltoni, O. Mattelaer, T. Stelzer, JHEP 1106 (2011) 128.

[21] H. Murayama, I. Watanabe, K. Hagiwara, KEK-91-11.

[22] K. Hagiwara, J. Kanzaki, Q. Li, K. Mawatari, Eur. Phys. J. C56 (2008) 435.

[23] P. de Aquino, K. Hagiwara, Q. Li, F. Maltoni, JHEP 06 (2011) 132.

[24] A. D. Martin, W. J. Stirling, R. S. Thorne, and G. Watt, Eur. Phys. J. C63 (2009) 189.